New Intermediates for the Synthesis of Olefin Polymerization Catalysts: the Complexes $[M_2(\mu\text{-}Cl)_2Cl_4(thf)_4]$ (M = Ti or V, thf = tetrahydrofuran); Crystal Structures and Properties†

Piotr Sobota,* Jolanta Ejfler, Sławomir Szafert, Krzysztof Szczegot and Wanda Sawka-Dobrowolska
Institute of Chemistry, University of Wrocław, 14 F. Joliot-Curie, 50-383 Wrocław, Poland

---

The dimeric titanium(III) and vanadium(III) complexes $[M_2(\mu\text{-}Cl)_2Cl_4(thf)_4]$ (M = Ti **1** or V **2**, thf = tetrahydrofuran) have been prepared by recrystallization of $[MCl_3(thf)_3]$ from dichloromethane. In the dimers, composed of slightly distorted edge-sharing octahedra, the metal atoms separated by Ti ⋯ Ti and V ⋯ V distances of 3.711(3) and 3.619(1) Å, respectively, are surrounded by two terminal Cl atoms, two oxygen atoms of thf molecules and are linked by two bridging Cl atoms. The geometry around the titanium atoms differs from that around vanadium because the thf molecules and the terminal chlorine atoms are differently located with respect to the bridging chlorine atoms of the $M_2(\mu\text{-}Cl)_2$ unit. High catalytic activity was found for ethylene polymerization by **1**.

Bimetallic complexes containing titanium, magnesium and electron-donor molecules supported on SiO_2, when combined with aluminium alkyls, show high catalytic activity in ethylene polymerization.[1,2] The titanium–magnesium halide complexes $[Mg_2(\mu\text{-}Cl)_3(thf)_6][TiCl_5(thf)]$[3] and $[(MeCO_2Et)_4Mg(\mu\text{-}Cl)_2TiCl_4]$[4] can be prepared by treating $TiCl_4$ and $MgCl_2$ in tetrahydrofuran (thf) or ethyl acetate, respectively. The mechanism by which $MgCl_2$ enhances catalyst activity is frequently attributed to the similar layer-lattice structure of magnesium dichloride and titanium trichloride.[5–7]

Supported vanadium catalyst, in the presence of halogenocarbons as promoters, displays high activity. Addition of $MgCl_2$ to the supported VCl_3 precursor did not significantly raise catalytic activity, and therefore was a non-essential component.[8] The role of the activator was not known. It was suggested that halogenocarbons oxidize inactive vanadium(II) to vanadium(III), which is in turn reduced to the inactive II state during chain termination.[9] Recently, Karol *et al.*[8] have shown that this seems doubtful and strongly indicate that the divalent vanadium centre comprises the active site. Studies with bimetallic vanadium–zinc complexes, $[(thf)_4V(\mu\text{-}Cl)_2ZnCl_2]$,[10] $[VCl_2(thf)_4][ZnCl_3(thf)]$,[10] and $[V_2(\mu\text{-}Cl)_3(thf)_6][Zn_2(\mu\text{-}Cl)_2Cl_4]$[11] do not give clear correlations between structure and polymerization activity.

We describe here a new simple high-yield method of synthesis leading to $[M_2(\mu\text{-}Cl)_2Cl_4(thf)_4]$ (M = Ti **1** or V **2**) compounds *via* recrystallization of $[MCl_3(thf)_3]$ from CH_2Cl_2 and report the details of their crystal structures.

Results and Discussion

Synthesis and Structure of $[Ti_2(\mu\text{-}Cl)_2Cl_4(thf)_4]$.—There is a lack of titanium(III) species soluble in non-aqueous solvents and suitable as starting materials for the preparation of the modern high-activity polyethylene $MgCl_2$–$TiCl_3$ catalyst.[1,2] The most widely used is $[TiCl_3(thf)_3]$ which is prepared[3] according to reaction (1). The reduction of $[TiCl_4(thf)_2]$ in the presence of a stoichiometric amount of thf with excess of aluminium turnings in CH_2Cl_2 yields green crystals of composition $TiCl_3{\cdot}2thf$ **1** [equation (2)]. Species **1** is probably formed directly from $[TiCl_3(thf)_3]$ in CH_2Cl_2. When $[TiCl_3(thf)_3]$ was dissolved in dichloromethane and the solution was stirred under N_2 until the colour changed from blue to green, green needle-shaped crystals of **1** were obtained. Compound **1** is very reactive, immediately decomposing on exposure either to air or moisture, but is stable under N_2. It is soluble in halogenated solvents, and unstable in thf because the titanium atom easily undergoes solvation and the complex $[TiCl_3(thf)_3]$ is formed immediately [equation (3)].[12]

$$3[TiCl_4(thf)_2] + Al \xrightarrow{thf} 3[TiCl_3(thf)_3] + [AlCl_3(thf)_2] \quad (1)$$

$$6[TiCl_4(thf)_2] + 2Al + 4thf \xrightarrow{CH_2Cl_2} 3[Ti_2(\mu\text{-}Cl)_2Cl_4(thf)_4] + 2[AlCl_3(thf)_2] \quad (2)$$

$$\underset{\text{blue}}{2[TiCl_3(thf)_3]} \underset{+2thf}{\overset{CH_2Cl_2,\ -2thf}{\rightleftharpoons}} 2[TiCl_3(thf)_2] \rightleftharpoons \underset{\text{green}}{[Ti_2(\mu\text{-}Cl)_2Cl_4(thf)_4]} \quad (3)$$

The five-co-ordinate complex $[TiCl_3(thf)_2]$ is probably an intermediate in the formation of dimeric **1** according to the dissociation mechanism in equation (3). The dimerization of **1** occurs through chloride bridges to compensate for the lack of electron density on the titanium atoms. Thermal decomposition of $[TiCl_3(thf)_3]$ also leads to the five-co-ordinated compound $[TiCl_3(thf)_2]$.[13] The IR spectrum shows the expected bands due to ν(COC) and sharp bands at 354 vs and 292vs cm^{-1} attributed to ν(Ti–Cl) which are shifted to lower wavenumbers compared to ν(Ti–Cl) 360vs, 330vs and 300m cm^{-1} for $[TiCl_3(thf)_3]$.[13] The magnetic susceptibility of **1** was determined between 4.2 and 293 K giving μ_B 1.64 and 1.35 per titanium atom, respectively. These values do not correspond to 0.43 and 1.43 μ_B found for the antiferromagnetic dimer $[Ti_2(\mu\text{-}Cl)_2Cl_4\{C_6H_4(CO_2Et)_2\text{-}o\}_2]{\cdot}4CH_2Cl_2$.[14] A best fit for J was impossible to obtain for **1** using a model based on the exchange Hamiltonian $-2S_1S_2$ where $S_1 = S_2 = \frac{1}{2}$. The only EPR parameter recorded was the trivial isotropic g value of a single-line signal, which belongs to an $S = \frac{1}{2}$ impurity of 1% Ti^{3+}. Therefore 99% of Ti^{3+} is EPR-silent. A similar effect was observed with $[Ti_2(\mu\text{-}Cl)_2Cl_4\{C_6H_4(CO_2Et)_2\text{-}o\}_2]{\cdot}4CH_2Cl_2$.[14]

The magnetic properties, IR spectra and stoichiometry

---

† *Supplementary data available:* see Instructions for Authors, *J. Chem. Soc., Dalton Trans.*, 1993, Issue 1, pp. xxiii–xxviii.

Table 1 Principal interatomic distances (Å) and bond angles (°) for complex **1**

Ti(1)–Cl(1)	2.470(2)	Ti(2)–Cl(1)	2.490(2)
Ti(1)–Cl(2)	2.335(2)	Ti(2)–Cl(3)	2.327(2)
Ti(1)–O(2)	2.099(6)	Ti(2)–O(1)	2.082(4)
O(2)–C(5)	1.448(13)	O(1)–C(1)	1.450(9)
O(2)–C(6)	1.383(13)	O(1)–C(2)	1.470(8)
C(5)–C(7)	1.371(18)	C(1)–C(3)	1.488(10)
C(6)–C(8)	1.381(19)	C(2)–C(4)	1.443(12)
C(7)–C(8)	1.413(18)	C(3)–C(4)	1.448(12)
Ti(1) ··· Ti(2)	3.711(3)		
Cl(1)–Ti(1)–O(2)	92.0(2)	Cl(1)–Ti(2)–O(1)	87.5(2)
Cl(1)–Ti(1)–O(2′)	175.1(2)	Cl(1)–Ti(2)–O(1′)	86.7(2)
Cl(1)–Ti(1)–Cl(1′)	83.5(1)	Cl(1)–Ti(2)–Cl(1′)	82.7(1)
Cl(1)–Ti(1)–Cl(2)	90.5(1)	Cl(1)–Ti(2)–Cl(3)	90.7(1)
Cl(1)–Ti(1)–Cl(2′)	92.1(1)	Cl(1)–Ti(2)–Cl(3′)	173.4(1)
Cl(2)–Ti(1)–Cl(2′)	176.6(1)	Cl(3)–Ti(2)–Cl(3′)	95.9(1)
Cl(2)–Ti(1)–O(2)	90.0(2)	Cl(3)–Ti(2)–O(1)	92.5(2)
Cl(2)–Ti(1)–O(2′)	87.6(2)	Cl(3)–Ti(2)–O(1′)	92.7(2)
O(2)–Ti(1)–O(2′)	92.5(3)	O(1)–Ti(2)–O(1′)	172.3(2)
O(2)–Ti(1)–Cl(1′)	175.1(2)	O(1)–Ti(2)–Cl(1′)	86.7(2)
O(2)–Ti(1)–Cl(2′)	87.6(2)	O(1)–Ti(2)–Cl(3′)	92.7(2)
Ti(1)–Cl(1)–Ti(2)	96.9(1)		
O(2)–C(5)–C(7)	107.2(10)	O(1)–C(1)–C(3)	106.7(6)
C(5)–C(7)–C(8)	110.0(12)	C(1)–C(3)–C(4)	106.0(8)
C(7)–C(8)–C(6)	105.4(12)	C(3)–C(4)–C(2)	110.8(8)
C(8)–C(6)–O(2)	111.6(11)	C(4)–C(2)–O(1)	105.6(7)
C(6)–O(2)–C(5)	105.2(8)	C(2)–O(1)–C(1)	109.6(5)

Primed atoms are related to unprimed ones by $-x, y, \frac{1}{2} - z$.

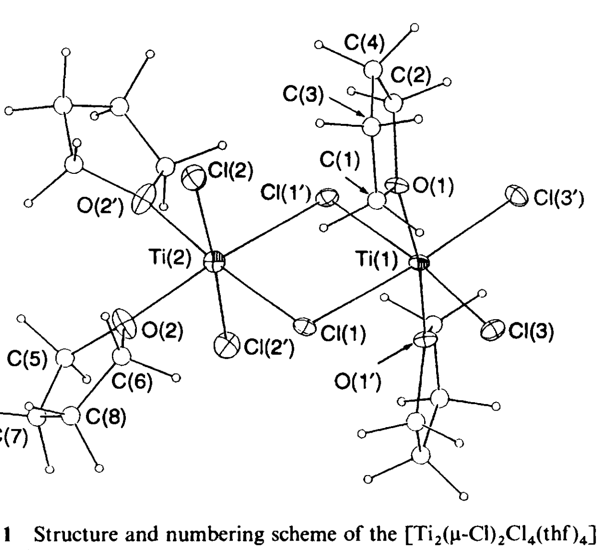

Fig. 1 Structure and numbering scheme of the $[Ti_2(\mu-Cl)_2Cl_4(thf)_4]$ molecule

suggested that compound **1** was a dimeric species. This formulation was confirmed by a crystal structure study. The results are presented in Table 1 and Fig. 1. The titanium atoms are surrounded by two terminal chlorine atoms, two bridging chlorine atoms and two oxygen atoms of thf molecules to form a slightly distorted edge-sharing dioctahedron. The general geometry around Ti(1) differs from that of Ti(2). The O(1) oxygen atom is situated *trans* to O(1′) and both are *cis* to bridging chlorine atoms, while O(2) and O(2′) are situated *trans* to bridging chlorine atoms Cl(1′) and Cl(1), respectively. This feature differentiates molecule **1** from the dimeric, centrosymmetric complex $[Ti_2(\mu-Cl)_2Cl_4\{C_6H_4(CO_2Et)_2\text{-}o\}_2]$ where two carbonyl oxygen atoms of the co-ordinated diethyl *o*-phthalate ester molecules are located *cis* and *trans* to the bridging chlorine atoms of the $Ti(\mu-Cl)_2Ti$ unit. It is worthy of note that similar zirconium $[Zr_2(\mu-Cl)_2Cl_4(PBu_3)_4]$ and hafnium $[Hf_2(\mu-Cl)_2Cl_4(PEt_3)_4]$ dimers[15–17] have the phosphine ligands located only *trans* to the two bridging chlorine atoms.[17] The Ti–Cl(terminal), Ti–Cl(bridge) and Ti–O bond lengths in **1** and in $[Ti_2(\mu-Cl)_2Cl_4\{C_6H_4(CO_2Et)_2\text{-}o\}_2]$ are comparable but the Ti–Cl$_b$–Ti bond angles 96.9(1) and 94.7(1)° and Ti ··· Ti bond distances of 3.711(3) and 3.629(4) Å, respectively are slightly different.

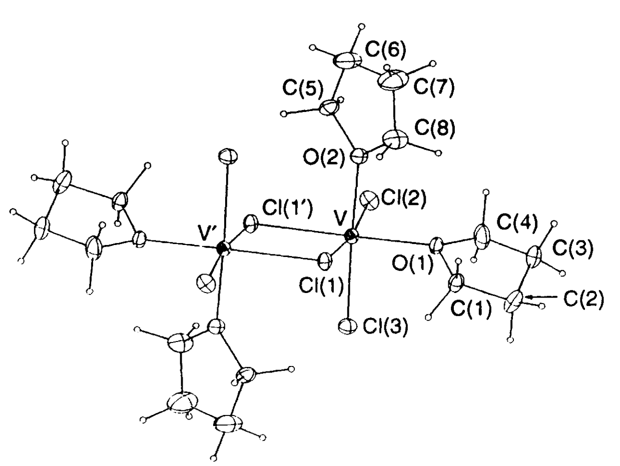

Fig. 2 Structure and numbering scheme of the $[V_2(\mu-Cl)_2Cl_4(thf)_4]$ molecule

Polymerization Studies.—The results of ethylene polymerization tests on $[Ti_2(\mu-Cl)_2Cl_4(thf)_4]$ and six related compounds are shown in Table 5. The catalysts were prepared by milling a hexane slurry of $[MgCl_2(thf)_2]$ and one of the compounds listed. Triethylaluminium was the cocatalyst. The highest activities were obtained with **1** and $[Ti_2(\mu-Cl)_2Cl_4\{C_6H_4(CO_2Et)_2\text{-}o\}_2]$ dimeric species, 131.2 and 126.7 kg polyethylene per g Ti h^{-1} respectively. Instead, only 21 kg polyethylene per g Ti h^{-1} were obtained under the same conditions when monomeric $[TiCl_3(thf)_3]$ was used as a precatalyst. Hence it follows that the propagation constant for ethylene polymerization on a bimetallic catalyst centre is probably much larger than on a mononuclear titanium centre. It is difficult to say at the moment whether the $[Ti_2(\mu-Cl)_2Cl_4(thf)_4]$–$MgCl_2$ catalyst is similar to the commercial Yamaguchi/Mitsubishi Chemical $MgCl_2$–$TiCl_3$–thf catalyst.[1] We supposed that the dimer structure is maintained in the **1**–$MgCl_2$ catalyst assembly. Note that the reaction between $TiCl_4$ and $MgCl_2$ in thf yields a yellow crystalline salt $[Mg_2(\mu-Cl)_3(thf)_6][TiCl_5(thf)]$,[3] which together with the organoaluminium cocatalyst is used as a commercial catalyst.[1,8]

Synthesis and Structure of $[V_2(\mu-Cl)_2Cl_4(thf)_4]$.—Our efforts to prepare the dimeric vanadium compound $[V_2(\mu-Cl)_2Cl_4(thf)_4]$ similar to **1** have been successful. When $[VCl_3(thf)_3]$ was dissolved in CH_2Cl_2 and the deep red solution exposed to slow diffusion of hexane a red needle-shaped crystalline solid of composition $VCl_3{\cdot}2thf$ **2** was formed. Compound **2**, like **1**, immediately decomposes in air, is well soluble in halogenated solvents and in thf the complex $[VCl_3(thf)_3]$ is formed immediately. The IR spectrum shows bands due to ν(COC) and broad bands at 310s, 340s and 355 cm^{-1} attributed to ν(V–Cl). The complex as a solid shows bands at 13 333 and 22 707 cm^{-1} in its diffuse reflectance spectrum, close to the values of 12 933 and 21 739 cm^{-1} observed in CH_2Cl_2 solution. Those bands can be assigned to the $^3T_{1g}(F) \longrightarrow {}^3T_{2g}(F)$ and $^3T_{1g}(F) \longrightarrow {}^3T_{1g}(P)$ transitions respectively for co-ordinated d^2 species, *cf.* $[VCl_2(H_2O)_4]Cl$,[18] $[VCl_2(ROH)_4]Cl$[19] (R = alkyl) and $[VCl_2(MeCN)_4][SbCl_6]$.[20] The electronic spectra suggest that the compound has similar structures in solution and in the solid state.

The results of an X-ray diffraction study are presented in Table 2 and Fig. 2. In the crystalline state compound **2** is composed of discrete molecules of $[V_2(\mu-Cl)_2Cl_4(thf)_4]$. The

Table 2 Principal interatomic distances (Å) and bond angles (°) for complex **2**

V–Cl(1)	2.424(1)	V–O(1)	2.057(2)
V–Cl(2)	2.300(1)	V–O(2)	2.043(2)
V–Cl(3)	2.292(1)	V···V′	3.619(1)
V–Cl(1′)	2.440(1)		
O(2)–C(5)	1.464(4)	O(1)–C(1)	1.470(4)
O(2)–C(8)	1.459(4)	O(1)–C(4)	1.462(4)
C(5)–C(6)	1.483(6)	C(1)–C(2)	1.504(5)
C(6)–C(7)	1.439(8)	C(2)–C(3)	1.504(6)
C(7)–C(8)	1.429(8)	C(3)–C(4)	1.471(6)
Cl(1)–V–O(1)	174.22(8)	Cl(2)–V–O(2)	88.21(7)
Cl(1)–V–O(2)	90.41(7)	Cl(3)–V–Cl(1′)	91.62(4)
Cl(1)–V–Cl(2)	90.92(4)	Cl(3)–V–O(1)	89.78(7)
Cl(1)–V–Cl(1′)	83.85(4)	Cl(3)–V–O(2)	175.25(8)
Cl(1)–V–Cl(3)	92.71(4)	O(1)–V–O(2)	86.79(9)
Cl(2)–V–Cl(1′)	171.50(5)	O(1)–V–Cl(1′)	90.87(7)
Cl(2)–V–Cl(3)	95.32(5)	O(2)–V–Cl(1′)	85.14(7)
Cl(2)–V–O(1)	94.04(7)	V–Cl(1)–V′	96.15(4)
V–O(1)–C(1)	122.6(2)	V–O(2)–C(5)	125.7(2)
V–O(1)–C(4)	123.6(3)	V–O(2)–C(8)	125.3(3)
O(2)–C(5)–C(6)	106.0(4)	O(1)–C(1)–C(2)	105.0(3)
C(5)–C(6)–C(7)	106.7(5)	C(1)–C(2)–C(3)	104.7(4)
C(6)–C(7)–C(8)	110.1(5)	C(2)–C(3)–C(4)	104.0(4)
C(7)–C(8)–O(2)	106.3(4)	C(3)–C(4)–O(1)	106.3(4)
C(8)–O(2)–C(5)	109.0(3)	C(4)–O(1)–C(1)	109.1(3)

Primed atoms are related to unprimed ones by $-x$, $-y$, $1 - z$.

Table 3 Final atomic coordinates of non-hydrogen atoms with estimated standard deviations (e.s.d.s) in parentheses for complex **1**

Atom	*x*	*y*	*z*
Ti(1)	0	0.235 73(9)	0.25
Ti(2)	0	0.059 04(9)	0.25
Cl(1)	0.179 39(24)	0.148 00(9)	0.311 46(9)
Cl(2)	0.195 22(30)	0.239 04(11)	0.143 92(12)
Cl(3)	0.190 32(29)	−0.015 24(9)	0.313 47(11)
O(1)	0.166 6(6)	0.065 7(2)	0.153 1(2)
O(2)	0.159 0(9)	0.304 8(3)	0.310 1(3)
C(1)	0.363 3(10)	0.071 1(4)	0.157 5(4)
C(2)	0.100 4(11)	0.071 5(4)	0.069 9(4)
C(3)	0.424 3(12)	0.070 5(5)	0.074 2(4)
C(4)	0.261 2(13)	0.078 1(5)	0.024 1(4)
C(5)	0.099 0(17)	0.360 9(5)	0.351 7(7)
C(6)	0.339 4(14)	0.296 8(6)	0.334 5(9)
C(7)	0.236 0(17)	0.377 5(7)	0.405 3(8)
C(8)	0.390 1(17)	0.338 7(6)	0.394 6(8)

Table 4 Final atomic coordinates of non-hydrogen atoms with e.s.d.s in parentheses for complex **2**

Atom	*x*	*y*	*z*
V	0.021 88(9)	0.072 77(7)	0.682 55(6)
Cl(1)	0.217 85(13)	−0.055 06(11)	0.514 20(9)
Cl(2)	0.247 92(14)	0.051 26(12)	0.853 32(10)
Cl(3)	0.159 92(14)	0.310 51(11)	0.692 57(10)
O(1)	−0.169 0(3)	0.171 8(2)	0.810 7(2)
O(2)	−0.123 5(3)	−0.132 8(2)	0.671 8(2)
C(1)	−0.320 3(5)	0.260 6(4)	0.773 2(3)
C(2)	−0.345 5(6)	0.376 7(4)	0.904 3(4)
C(3)	−0.281 2(6)	0.306 5(4)	1.011 0(4)
C(4)	−0.122 8(7)	0.218 8(5)	0.958 2(4)
C(5)	−0.033 5(5)	−0.273 0(4)	0.659 6(4)
C(6)	−0.196 8(7)	−0.391 4(5)	0.653 3(5)
C(7)	−0.367 1(8)	−0.314 0(6)	0.683 3(7)
C(8)	−0.334 5(5)	−0.163 2(5)	0.675 4(5)

Table 5 Polymerization of ethylene with titanium–$MgCl_2$–$AlEt_3$ catalysts

Compound	Productivity/kg polyethylene per g Ti h^{-1}
$[TiCl_4(thf)_2]$	11.6
$[TiCl_3(thf)_3]$	21.1
$[Ti_2(\mu\text{-}Cl)_2Cl_4(thf)_4]$	131.2
$[Ti_2(\mu\text{-}Cl)_2Cl_4\{C_6H_4(CO_2Et)_2\text{-}o\}_2]$	126.7
$[Mg(thf)_6][TiCl_5(thf)]_2$	16.9
$[Mg_2(\mu\text{-}Cl)_3(thf)_6][TiCl_5(thf)]$	12.1
$[(thf)_4Mg(\mu\text{-}Cl)_2TiCl_4]$	36.1

Polymerization conditions: $[Ti]_0 = 0.01$ mmol dm^{-3}; Al:Ti = 120:1, Mg:Ti = 10:1; $P_{ethylene} = 0.5$ MPa; in hexane.

molecule consists of two somewhat distorted octahedra sharing a common edge. Each vanadium(III) ion is octahedrally co-ordinated by two terminal chlorine atoms, two bridging chlorine atoms and two oxygen atoms of two tetrahydrofuran ligands. The two thf molecules are located *cis* and *trans* to the two bridging chlorine atoms. The O(2) oxygen atom of the thf ligand is situated *trans* to Cl(3), while O(1) of the second thf molecule is *trans* to the bridging chlorine atom Cl(1). The V–Cl_b bond lengths of 2.424(1) and 2.440(1) Å are similar to V–Cl_b 2.477 Å in $[V_2(\mu\text{-}Cl)_3(thf)_6]^+$.[11] The terminal [V–Cl(2) and V–Cl(3)] distances [2.300(1) and 2.292(1) Å] are comparable to V–Cl bond lengths [2.333(1), 2.326(1) and 2.297(1) Å] in monomeric $[VCl_3(thf)_3]$.[21] The V–O(1) distance of 2.057(2) Å is slightly longer than V–O(2) 2.043(2) Å but similar to V–O distances [2.054(3), 2.069(3) and 2.102(3) Å] in $[VCl_3(thf)_3]$. The O–V–O bond angle of 86.8(1)° and Cl–V–Cl angles ranging from 83.9 to 95.3° are not much compressed from 90°. The vanadium–vanadium separation of 3.619(1) Å and the V–Cl_b–V angles of 96.15(4)° are much greater than the metal–metal bond length of 2.721(1) Å and the acute Ta–Cl_b–Ta angle of 67.4° in $[Ta_2(\mu\text{-}Cl)_2Cl_4(PMe_3)_4]$.[22] The rhomboid of vanadium atoms and bridging chlorides in **2** is planar, but this plane does not include the equatorial ligands [Cl(2) and Cl(2′) atoms and the oxygen atoms O(1) and O(1′) are displaced by ±0.27 and ±0.08 Å, respectively].

Compound **2** is paramagnetic with a temperature (4.2–293 K)-independent μ_{eff} of 2.72 μ_B per vanadium atom (a plot of $1/\chi$ against T gives a straight line passing through the origin). No EPR signal was observed in the solid state, which additionally confirms the vanadium(III) oxidation state ($S = 1$). On dissolution in CH_2Cl_2 a hyperfine EPR spectrum with sets of eight lines arising from interaction of the d^1 electron with a ^{51}V nucleus ($I = \frac{7}{2}$) was observed. A similar spectrum was recorded for $[VCl_3(thf)_3]$. We have compared the spectral parameters with those of VO^{2+} complexes.[23] They are similar, *i.e.* vanadium(III) was oxidized in pure dichloromethane to vanadium(IV). The CH_2Cl_2 is very effective at activating the vanadium compounds towards ethylene polymerization and the ratio of activator to vanadium species [10c] is in the range of 100–300:1. Therefore the explanation of the oxidation mechanism of vanadium(III) in **2** and $[VCl_3(thf)_3]$ by dichloromethane is important and is under investigation.

The catalytic activity of $[VCl_3(thf)_3]$ (176 kg polyethylene per g Ti h^{-1})[10c] with tetrachloro-1,2-difluoroethane as activator and $AlEt_3$ as cocatalyst is comparable with that of complex **1** (see Table 5).

Conclusions

The presented results show that the behaviours of $[MCl_3(thf)_3]$ (M = Ti or V) in dichloromethane are similar yielding dimeric compounds $[M_2(\mu\text{-}Cl)_2Cl_4(thf)_4]$. The compounds are not isomorphous. This, almost certainly, is the result of repulsions between axial substituents of the $M_2(\mu\text{-}Cl)_2$ unit. If bending back of the ligands alone cannot relieve the axial repulsions, the only option is to twist the end groups away from each other, as observed in **1** and **2**. The titanium and vanadium catalysts have different requirements to achieve high catalytic activity in ethylene polymerization.[8] Addition of $MgCl_2$ to $[Ti_2(\mu\text{-}Cl)_2Cl_4(thf)_4]$ is an important route to high activity. The EPR, IR and X-ray powder diffraction data provided strong evidence for the absence of complex formation between $MgCl_2$ and $TiCl_3$ in thf.[8,12,24] However, in non-polar solvents the molecular magnesium–transition metal compounds $[\{(\eta\text{-}C_5H_5)_2Ti(\mu\text{-}Cl)_2\}_2Mg(thf)_2]$, $[\{(\eta\text{-}C_5H_5)_2Ti(\mu\text{-}Cl)_2\}_2Mg_2(\mu\text{-}Cl)_2(thf)_4]$[25] and $[(thf)_3Mg(\mu\text{-}Cl)_3MoCl_2O]$[26] are formed. How the $MgCl_2$ is incorporated with **1** in the catalyst can only be answered by further studies. Instead, the supported vanadium catalyst requires a halogenated promoter to maintain high polymerization productivity.[8] The present data show that CH_2Cl_2 is necessary for bimetallic $[M_2(\mu\text{-}Cl)_2Cl_4(thf)_4]$ or polymetallic centre formation.

Experimental

All manipulations were carried out under dinitrogen by use of a standard Schlenk system and vacuum line. The compounds $TiCl_3$, VCl_3 and $AlEt_3$ were commercial materials; $[TiCl_3(thf)_3]$[27] and $[VCl_3(thf)_3]$[28] were prepared by reported procedures. Solvents were dried and purified by standard techniques. Magnetic susceptibilities were measured by the Faraday method within the temperature range 4.2–293 K. Corrections for diamagnetism were made with Pascal's constants.[29] The EPR spectra were obtained on an SE type X-band spectrometer. The spectral intensity of the titanium(III) species was measured quantitatively by comparing the doubly integrated spectra of compound **1** and that of a standard heptane solution of 2,2,6,6-tetramethylpiperidine-1-oxyl. The following spectrometers were used: Specord Perkin-Elmer 180 for IR and Beckman UV 5240 for UV/VIS spectroscopy.

Synthesis.—$[Ti_2(\mu\text{-}Cl)_2Cl_4(thf)_4]$ **1**. *Method* (*a*). To a solution of $[TiCl_4(thf)_2]$ (3.5 g, 10.0 mmol) and an excess of aluminium turnings (0.5 g) was added dropwise tetrahydrofuran (8.5 cm^3, 10.2 mmol) and stirred. Over 2 d the colour changed from yellow to green. The aluminium turnings were filtered off and hexane (50 cm^3) was added to the filtrate. After several minutes a green compound precipitated, and was filtered off and washed with hexane (3 × 5 cm^3). Yield 2.8 g (92%) (Found: Cl, 35.30; Ti, 15.90. $C_{16}H_{32}Cl_6O_4Ti_2$ requires Cl, 35.65; Ti, 16.05%). IR (Nujol): 292vs (br), 354vs (br), 370 (sh), 460w, 576m, 686m, 724s, 852vs (br), 924s, 962w, 1008vs and 1030s cm^{-1}. No UV/VIS (in CH_2Cl_2) and reflectance spectra were observed.

Method (*b*). The complex $[TiCl_3(thf)_3]$ (2 g, 5.4 mmol) was dissolved in CH_2Cl_2 (50 cm^3). The solution was stirred for *ca.* 1 h until the colour changed from blue to green. The solution was exposed to slow diffusion of hexane. After 24 h green needle-shaped crystals were filtered off and washed with hexane (3 × 5 cm^3). Microanalysis data, an IR spectrum and Weissenberg photography of the crystals were identical as for the compound obtained by method (*a*).

$[V_2(\mu\text{-}Cl)_2Cl_4(thf)_4]$ **2**. The complex $[VCl_3(thf)_3]$ (3 g, 8.1 mmol) was dissolved in CH_2Cl_2 (50 cm^3) and stirred for 1 h. The solution was exposed to slow diffusion of hexane. After 1 week red crystals settled out and were filtered off and washed with hexane (3 × 5 cm^3). Yield 1.8 g (90%) (Found: Cl, 35.10; V, 16.70. $C_{16}H_{32}Cl_6O_4V_2$ requires Cl, 35.25; V, 16.90%). μ_{eff} = 2.72 in the range 4.2–293 K. EPR: $g_1 = 2.23, g_2 = 2.16, g_3 = 2.09, g_4 = 2.02, g_5 = 1.95, g_6 = 1.89, g_7 = 1.82, g_8 = 1.76$. IR (Nujol): 310s, 340s, 355 (sh), 438w, 848vs (br), 922m, 960w, 1006vs and 1040m cm^{-1}.

Polymerizations.—A slurry of $[MgCl_2(thf)_2]$ (30 mmol) in hexane (50 cm^3) was milled under argon in a glass mill (capacity 250 cm^3, with 20 balls of diameter 5–15 mm) at room temperature for 6 h. Then a titanium compound (3 mmol) and hexane (50 cm^3) were added and the mixture was milled for 24 h. The sample of precatalyst suspension (containing 0.01 mmol titanium) was activated with $AlEt_3$ (20 mmol) for 15 min at 323 K under argon. The polymerization of ethylene was carried out at 323 K in a stainless-steel reactor (1 dm^3) equipped with a stirrer, in hexane at an ethylene pressure of 0.5 MPa. It was quenched with a 5% solution of HCl in methanol (150 cm^3), the polymer was filtered off, washed with methanol and dried under vacuum.

Crystallography.—*Crystal data*. $C_{16}H_{32}Cl_6O_4Ti_2$ **1**, green crystals, $M = 596.949$, monoclinic, space group $C2/c$, $a = 7.352(2)$, $b = 21.003(9)$, $c = 16.830(5)$ Å, $\beta = 92.21(2)°$, $U = 2596(2)$ Å^3, $D_m = 1.544$ g cm^{-3}, $Z = 4$, $D_c = 1.527(1)$ g cm^{-3}, $F(000) = 1224$, $T = 240.0(1)$ K, $\mu = 1.17$ mm^{-1}.

$C_{16}H_{32}Cl_6O_4V_2$ **2**, red crystals, $M = 603.029$, triclinic, space group $P\bar{1}$, $a = 6.863(2)$, $b = 9.285(7)$, $c = 10.513(7)$ Å, $\alpha = 107.99(6)$, $\beta = 96.75(4)$, $\gamma = 94.83(4)°$, $U = 627(1)$ Å^3, $D_m = 1.610$ g cm^{-3}, $Z = 1$, $D_c = 1.595(2)$ g cm^{-3}, $F(000) = 308$, $T = 230.0(1)$ K, $\mu = 1.32$ mm^{-1}.

Data collection and processing. Preliminary data were recorded by photographic methods. Intensities were collected using a Kuma KM4 four-circle diffractometer with an Oxford Cryosystem-Cryostream Cooler, in the ω–2θ mode (crystal dimensions 0.3 × 0.1 × 0.4 for **1** and 0.4 × 0.4 × 0.3 mm for **2**) with Mo-Kα radiation. For both crystals the intensities of three standard reflections, monitored every 50 intensity scans, showed no evidence of crystal decay. A total of 2558 ($4 < 2\theta < 56°$) and 1554 ($4 < 2\theta < 56°$) reflections were measured for **1** and **2**, respectively, from which 1134 and 1329 with $I > 3.0\sigma(I)$ were used for calculations. The structures were solved by the Patterson method and refined by full-matrix least-squares calculations using SHELX 76.[30] The hydrogen atoms were put in calculated positions with d(C–H) = 1.08 Å and introduced as fixed contributors in the final stage of refinement. A weighting scheme of the form $w = 1/\sigma^2(F_o)$ was applied for both structures. Final R $\{=[w(||F_o| - |F_c||)/\Sigma|F_o|\}$ and R' $\{=[\Sigma w(|F_o| - |F_c|)^2/\Sigma wF_o{}^2]^{\frac{1}{2}}\}$ values were 0.0470 and 0.0400 for **1** and 0.0251 and 0.0247 for complex **2**. The R_{int} value for **1** was 0.0301. For the last cycle of refinement the maximum value of the ratio Δ/σ was 0.059 for **1** and 0.107 for **2**. The final difference map showed a general background within −0.355 and 0.601 and −0.339 and 0.321 e Å^{-3} for **1** and **2**, respectively. The final positional parameters for the non-hydrogen atoms are given in Tables 3 and 4.

Additional material available from the Cambridge Crystallographic Data Centre comprises H-atom coordinates, thermal parameters and remaining bond lengths and angles.

References

1 U. Giannini, E. Albizzati, S. Parodi and F. Pirinoli, *U.S. Pat.*, 4 124 532, 1978; 4 174 429, 1979; K. Yamaguchi, N. Kanoh, T. Tanaka, N. Enokido, A. Murakami and S. Yoshida, *U.S. Pat.*, 3 989 881, 1976; F. J. Karol, G. L. Goeke, B. E. Wagner, W. A. Fraser, R. J. Jorgensen and N. Friis, *U.S. Pat.*, 4 302 566, 1981.
2 A. Greco, G. Bertolini and S. Cesca, *J. Appl. Polym. Sci.*, 1980, **25**, 2045.
3 P. Sobota, J. Utko and T. Lis, *J. Chem. Soc., Dalton Trans.*, 1984, 2077.
4 L. Brun, *Acta Crystallogr.*, 1966, **20**, 739.
5 V. A. Zakharov, G. D. Bukatov and Y. I. Yermakov, *Polym. Sci. Technol.*, 1983, **19**, 267.
6 G. D. Bukatov, S. H. Shepelev, V. A. Zakharov, S. A. Sergeev and Y. I. Yermakov, *Makromol. Chem.*, 1983, **183**, 2657.
7 A. A. Baulin, M. A. Budanova and S. S. Ivanchev, *Kinet. Catal.* (*Engl. Transl.*), 1982, **23**, 539.
8 F. J. Karol, K. J. Cann and B. E. Wagner, in *Transition Metals and Organometallics as Catalysts for Olefin Polymerization*, eds. W. Kaminsky and H. Sinn, Springer, Berlin, Heidelberg, 1988, p. 149.
9 D. L. Christman, *J. Polym. Sci., Part A-1*, 1972, **10**, 471.
10 (*a*) K. Folting, J. C. Huffman, R. L. Bansemer, K. G. Caulton, J. L. Martin and P. D. Smith, *Inorg. Chem.*, 1984, **23**, 4589; (*b*) K. Folting, J. C. Huffman, R. L. Bansemer and K. G. Caulton, *Inorg. Chem.*,

1984, **23**, 3289; (*c*) P. D. Smith, J. L. Martin, J. C. Huffman, R. L. Babsemer and K. G. Caulton, *Inorg. Chem.*, 1985, **24**, 2997.

11 A. F. Cotton, S. A. Duraj, L. E. Manzer and W. J. Roth, *J. Am. Chem. Soc.*, 1985, **107**, 3850; R. J. Bouma, J. H. Teuben, W. R. Beukema, R. L. Bansemer, J. C. Huffman and K. G. Caulton, *Inorg. Chem.*, 1984, **23**, 2715.

12 P. Sobota, *Polyhedron*, 1992, **11**, 715.

13 M. Handlovič, D. Mikloš and M. Zikmund, *Acta Crystallogr., Sect. B*, 1981, **37**, 811; M. Zikmund and L. Štepničková, *Chem. Zvesti*, 1969, **23**, 850; M. Kohútova and M. Zikmund, *Transition Met. Chem.*, 1992, **17**, 186.

14 P. Sobota, J. Ejfler, J. Utko and T. Lis, *J. Organomet. Chem.*, 1991, **410**, 149.

15 J. H. Wengrovius, R. R. Schrock and C. S. Day, *Inorg. Chem.*, 1981, **20**, 1844.

16 M. E. Riehl, R. S. Wilson and G. Girolami, *Inorg. Chem.*, 1993, **32**, 218; 1990, **29**, 3200.

17 F. A. Cotton, P. A. Kibala and W. A. Wojtczak, *Inorg. Chim. Acta*, 1990, **177**, 1; F. A. Cotton, W. Shang and W. A. Wojtczak, *Inorg. Chem.*, 1990, **29**, 313.

18 S. M. Horner and S. Y. Tyree, *Inorg. Chem.*, 1964, **3**, 1173.

19 A. T. Casey and R. J. H. Clark, *Inorg. Chem.*, 1969, **8**, 1216.

20 P. P. K. Claire, G. R. Willey and M. G. B. Drew, *J. Chem. Soc., Chem. Commun.*, 1987, 1100.

21 F. A. Cotton, S. A. Duraj, G. L. Powell and W. J. Roth, *Inorg. Chim. Acta*, 1986, **113**, 81.

22 A. P. Sattelberger, R. B. Wilson and J. C. Huffman, *Inorg. Chem.*, 1982, **21**, 2396.

23 A. Jezierski and J. B. Raynor, *J. Chem. Soc., Dalton Trans.*, 1981, 1.

24 P. Sobota and J. Utko, *Polymer Commun.*, 1988, **29**, 144.

25 D. W. Stephan, *Organometallics*, 1992, **11**, 996.

26 P. Sobota, J. Ejfler, T. Płuziński and T. Lis, *Polyhedron*, 1991, **10**, 2457.

27 W. Schofer and K. H. Thiele, *Z. Anorg. Allg. Chem.*, 1971, **381**, 205.

28 L. E. Manzer, *Inorg. Synth.*, 1982, **21**, 138.

29 A. Earnshaw, *Introduction to Magnetochemistry*, Academic Press, London, 1986, p. 5.

30 G. M. Sheldrick, SHELX 76, Program for Crystal Structure Determination, University of Cambridge, 1976.

Received 29th March 1993; *Paper* 3/01801F